NRC Publications Archive
Archives des publications du CNRC

A new technique for measuring retrograde vitrification in polymer-gas systems and for making ultramicrocellular foams from the retrograde phase

Handa, Y. Paul; Zhang, ZhiYi

This publication could be one of several versions: author's original, accepted manuscript or the publisher's version. / La version de cette publication peut être l'une des suivantes : la version prépublication de l'auteur, la version acceptée du manuscrit ou la version de l'éditeur.
For the publisher's version, please access the DOI link below./ Pour consulter la version de l'éditeur, utilisez le lien DOI ci-dessous.

Publisher's version / Version de l'éditeur:
https://doi.org/10.1002/(SICI)1099-0488(20000301)38:5<716::AID-POLB9>3.0.CO;2-N
Journal of Polymer Science B: Polymer Physics, 38, 5, pp. 716-725, 2000

NRC Publications Record / Notice d'Archives des publications de CNRC:
https://nrc-publications.canada.ca/eng/view/object/?id=644d6b2f-32a5-4c5c-8565-3cfd59be6c50
https://publications-cnrc.canada.ca/fra/voir/objet/?id=644d6b2f-32a5-4c5c-8565-3cfd59be6c50

Access and use of this website and the material on it are subject to the Terms and Conditions set forth at
https://nrc-publications.canada.ca/eng/copyright
READ THESE TERMS AND CONDITIONS CAREFULLY BEFORE USING THIS WEBSITE.

L'accès à ce site Web et l'utilisation de son contenu sont assujettis aux conditions présentées dans le site
https://publications-cnrc.canada.ca/fra/droits
LISEZ CES CONDITIONS ATTENTIVEMENT AVANT D'UTILISER CE SITE WEB.

Questions? Contact the NRC Publications Archive team at PublicationsArchive-ArchivesPublications@nrc-cnrc.gc.ca. If you wish to email the authors directly, please see the first page of the publication for their contact information.

Vous avez des questions? Nous pouvons vous aider. Pour communiquer directement avec un auteur, consultez la première page de la revue dans laquelle son article a été publié afin de trouver ses coordonnées. Si vous n'arrivez pas à les repérer, communiquez avec nous à PublicationsArchive-ArchivesPublications@nrc-cnrc.gc.ca.

National Research Council Canada
Conseil national de recherches Canada
Canada

A New Technique for Measuring Retrograde Vitrification in Polymer–Gas Systems and for Making Ultramicrocellular Foams from the Retrograde Phase

Y. PAUL HANDA, ZHIYI ZHANG

Institute for Chemical Process and Environmental Technology, National Research Council of Canada, Ottawa, Ontario, Canada K1A 0R6

Received 15 June 1999; revised 28 September 1999; accepted 6 December 1999

ABSTRACT: A stepwise temperature- and pressure-scanning thermal analysis method was developed to measure glass-transition temperature T_g in the two-phase polymer–gas systems as a function of gas pressure p, and was used to confirm recent theoretical predictions that certain polymer–gas systems exhibit retrograde vitrification, that is, they undergo rubber-to-glass transition on heating. A complete T_g-p profile delineating the glass–rubber phase envelope was established for the PMMA-CO_2 system. The retrograde vitrification behavior observed, where at certain gas pressures the polymer exists in the rubbery state at low and high temperatures and in the glassy state at intermediate temperatures, was similar to that reported previously based on the creep-compliance measurements. The existence of the rubbery state at low temperatures was used to generate foams by saturating the polymer with CO_2 at 34 atm and at temperatures in the range −0.2 to 24 °C followed by foaming at temperatures in the range 24 to 90 °C. Foams with very fine cell structure never reported before could be prepared by this technique. For example, PMMA foams with average cell size of 0.35 μm and cell density of 4.4×10^{13} cells/g were prepared by processing the low temperature rubbery phase. © 2000 John Wiley & Sons, Inc. J Polym Sci B: Polym Phys 38: 716–725, 2000

Keywords: polymer; plasticization; gas; foams

INTRODUCTION

Compressed gases near or slightly above their critical points can dissolve to considerable extents in a glassy polymer causing a significant depression in the glass-transition temperature, T_g, of the polymer. This plasticization effect plays an important role in various areas including polymer membranes for gas separation;[1] extraction of unreacted species[2] or impurities[3] from polymers; incorporation of additives into polymers;[4,5] enhancing polymer–polymer miscibility;[6] and facilitating making polymer blends or composites,[7] polymer morphology modification,[8] and fabrication of cellular polymers or polymer foams.[9,10] For these applications, it is important to know the relationship between the polymer's T_g and the gas pressure, p, that is, the T_g-p profile. For example, in developing processes for making polymer foams, a knowledge of the T_g-p profile provides information on the conditions under which cell nucleation takes place, how the cellular morphology can be arrested, and the rheology of the polymer–gas system.

Over a limited pressure range, the T_g of a polymer–gas system usually changes linearly with the gas pressure, as revealed by the results for a number of systems including polystyrene-CO_2, PS-ethylene, PS-HFC134a,[8,11–13] polycarbonate-

Correspondence to: Y. P. Handa (E-mail: paul.handa@nrc.ca)

Journal of Polymer Science: Part B: Polymer Physics, Vol. 38, 716–725 (2000)
© 2000 John Wiley & Sons, Inc.

CO_2,[13,14] PVC-CO_2,[13] PET-CO_2,[15] and PMMA-CO_2.[14,16] However, for the latter system, it was reported[17] that at a CO_2 pressure of 39 atm, the system exhibited two T_g's—a lower $T_{g,l}$ at a temperature of 32.7 °C and a higher $T_{g,h}$ at a temperature of 58.8 °C. This observation was later on accounted for by the theoretical models,[18,19] which predicted that at a certain constant gas pressure or solubility, the polymer existed in the liquid (i.e., rubbery) state at temperatures below $T_{g,l}$ and above $T_{g,h}$, and in the glassy state at temperatures in between $T_{g,l}$ and $T_{g,h}$. The existence of $T_{g,l}$ is attributed to enhanced solubility of the gas at lower temperatures. This unusual behavior was termed retrograde vitrification[18] because, on heating under certain pressures, the polymer–gas system first exhibits a liquid-to-glass transition and then a glass-to-liquid transition. All the retrograde data reported in the literature on PMMA-CO_2 system were obtained by creep compliance measurements.[17,20] In addition to PMMA-CO_2, similar vitrification behavior was also found in the poly(ethyl methacrylate)-CO_2 system, again by creep compliance measurements.[21]

A number of techniques have been used to measure T_g in polymer–gas systems.[12,13] Of these, creep compliance is the only technique successfully used to establish the retrograde behavior. We tried the other *in situ* techniques of high-pressure calorimetry[12,16] and high-pressure DSC[8,13,15] to measure the retrograde profile, but failed. The major reason that the temperature-scanning techniques are not well suited for such measurements is that it is not possible to keep the polymer–gas system in thermodynamic equilibrium during the heating or cooling runs. The glass transition is characterized by a constant pressure heat capacity C_p step-change. The precision in heat capacities determined using a DSC is often quite poor but can be improved considerably by using the stepwise heating or the enthalpy increment method.[22] We have extended the stepwise C_p technique to the two-phase polymer–gas system to establish the C_p step and, thereby, determine the T_g of the system. Furthermore, the stepwise technique ensures that the thermodynamic equilibrium between polymer and gas is maintained throughout the measurements. In this article, we describe the stepwise C_p technique and show how it can be used to establish the T_g-p profile accurately and more efficiently than the creep compliance technique.

Cellular polymers with closed cells about 10 μm in size and a cell density of 10^8 cells/cm^3 are called microcellular foams[23] and those with cells less than 1 μm in size and cell density greater than 10^{12} cells/cm^3 are called ultramicrocellular (sometimes also called supermicrocellular) foams.[24] These cellular polymers are made by saturating the polymer with a compressed gas and then subjecting the system to thermodynamic instability by either rapidly increasing the temperature or decreasing the pressure, causing the dissolved gas to escape. Provided that the polymer is above its plasticized T_g under such a treatment, the escaping gas leaves behind a cellular structure whose characteristics, cell size, and cell density depend on the temperature and pressure conditions under which the polymer was treated with the gas. In the various foaming methods reported in the open and patent literature, the processing of the polymer by the temperature increase or pressure drop is done above $T_{g,h}$. In terms of the retrograde behavior, the polymer below $T_{g,l}$ is in the same state as that above $T_{g,h}$ and, so, it should be possible to produce micro- or ultramicrocellular foams below $T_{g,l}$. There are some other considerations that make foaming below $T_{g,l}$ attractive: at low temperatures, the gas solubility may be quite high at relatively low pressures and the high dissolved-gas content may give a high cell density; the low temperature may facilitate better control on cell growth and may lead to much finer cells; and processing at low pressures can circumvent the safety and equipment cost concerns. In this article, we report on foaming PMMA below $T_{g,l}$ using CO_2 as the blowing agent.

EXPERIMENTAL

PMMA from Canus Plastics was analyzed using GPC (Waters SEC equipped with a 401 DRI); it had M_w = 108,500 and M_n = 56,700. PMMA films around 300-μm thick and sheets around 1.25 mm were obtained by compression molding at 180 °C and then air quenched. High purity, bone dry CO_2 was used.

Setaram DSC121 was used for stepwise heat capacity measurements. Its temperature and energy scales were calibrated by measuring the heat capacities (in the stepwise mode, described below) of sapphire over the range of −40 to 140 °C, and by measuring, in the scanning mode, the melting points and heats of melting of high purity gallium, indium, tin, and zinc. The calibrations were

then tested by conducting stepwise heat capacity measurements on benzoic acid (SRM 39i from NIST). The technique for making high-pressure measurements with the DSC121 has been described elsewhere.[13] After installing the polymer film sample, the system was evacuated for a few hours to degas the polymer, and then both the reference and the measurement cells were pressurized to the desired pressure, p, monitored by a Setra pressure transducer (Model 204). The sample was held at a desired temperature in the range of −10 to 20 °C and sufficient time allowed for the polymer to attain equilibrium gas solubility.

Heat capacity measurements on the polymer–gas system were then made in the stepwise temperature or pressure-scanning mode. In the stepwise temperature scanning technique, the sample was held isothermally for 15 min to establish a baseline at the initial temperature T_i, then scanned at a rate of 1 °C/min to give a temperature jump of from 1 to 4 °C, and then held isothermally again for 15 min to establish a baseline at the final temperature T_f. These stepwise temperature jumps were continued until the desired temperature range was covered. The entire procedure was repeated with both reference and measurement cells containing the gas only at the same pressure as in the run with the polymer–gas system. Typical examples of the stepwise scans in the temperature range 0–12 °C are shown in Figure 1 for the sample (PMMA + CO_2) at 34 atm and the blank run with CO_2 at the same pressure. Also shown in Figure 1 are the corrected steps obtained by subtracting the blank run from the sample run. Integration of the peak for a given step yields the enthalpy increment ΔH required to affect the corresponding temperature change, T_f–T_i, and these two quantities then give, at the temperature $(T_f + T_i)/2$, the heat capacity C_p of the polymer containing dissolved gas. It should be noted that, in our setup, the gas phase volume was much larger than the volume of the DSC cells such that during the temperature scan the pressure in the system remained constant. The T_g of the polymer–gas system was obtained from the C_p-T data (see below), and the entire procedure was repeated at several gas pressures in order to establish the T_g-p profile.

In the stepwise pressure-scanning technique, the polymer was equilibrated with the gas at a pressure p and a temperature jump made from T_i to T_f. The system was then cooled back to T_i, the pressure was increased to the next value, and the

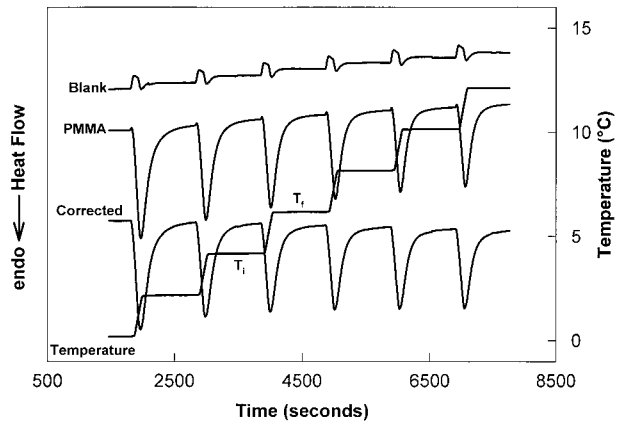

Figure 1. Representative plots of the stepwise DSC scans conducted under a CO_2 pressure of 34 atm and from 0–12 °C. Each temperature jump (T_f–T_i) was 2 °C, made at the rate of 1 °C/min. Isothermal hold before and after the jump was 15 min. The corrected thermogram was obtained by subtracting the blank run from the PMMA run.

temperature jump from T_i to T_f was made again once the polymer had equilibrated again with the new pressure. The system was cooled back to T_i and the temperature jumps, from T_i to T_f, continued at increasing pressures to obtain the C_p-p curve, which then gave the plasticization pressure p_g at $(T_f + T_i)/2$. The precision in T_g, measured by stepwise temperature or pressure jump, was ±1 °C.

For comparison, T_g measurements were also made by equilibrating the polymer sample with the gas at a given pressure and temperature and then scanning the system at 5 °C/min. The details of the temperature scanning technique to establish the T_g-p profile are given elsewhere.[13]

For solubility measurement at a given temperature and pressure, a known mass of the 1.25-mm thick PMMA sheet was first degassed for a few hours and then contacted with CO_2 in a pressure vessel made up of VCR fittings. The polymer sample was taken out periodically and weighed to ±0.1 mg until a constant mass was obtained. The total time taken for releasing the pressure, taking the sample out, and for weighing was within 1 min. Below the critical temperature of CO_2, solubility measurements were made by contacting the polymer with CO_2 in the compressed vapor or liquid state. The agreement between the solubility results obtained by dissolving CO_2 from the vapor or liquid phase was within ±1.5%. Glassy polymers usually undergo irreversible dilation on exposure to high pressure CO_2.[25] As a result, a

fresh sample was used for each pressure investigated.

For foaming, the polymer sheets were conditioned with compressed vapor or liquid CO_2 in the pressure vessel at the given temperature and pressure for 24 h, a time long enough to ensure establishment of the polymer–gas equilibrium. The pressure was then quickly released and samples brought to ambient conditions or transferred to a water bath held at various temperatures for foaming, followed by rapid quenching in ice-water slurry. The foaming time in water bath was 2 min, and the foams thus obtained were kept for at least 10 days prior to further analysis. The foam densities were measured by weighing the samples in air and in water. For microstructural analysis, a scanning electron microscope SEM (JEOL, JSM-5300) was used to take pictures of freshly exposed surfaces of foam samples fractured at liquid nitrogen temperature and then sputter coated with a thin layer of gold. The cells in the microphotographs were outlined manually and then rescanned into the computer for image analysis using the Image Pro Plus software from Media Cybernetics. For image analysis, the background of each scanned photograph was adjusted so that only the colored cells were visible on the monitor. All cellular characteristics such as equivalent diameter, perimeter, and area, and their distributions in each sample were obtained from the analysis, and the average cell size and cell density for a given foam sample were determined as described before.[10]

RESULTS AND DISCUSSION

Measurement of the Retrograde Profile

Heat capacities of neat PMMA at various temperatures measured by the stepwise technique are shown in Figure 2, and compared with data from the literature.[26] The agreement between the two sets of results is quite satisfactory, especially in the pre- and post-glass transition regions. A step increase in heat capacity with onset temperature of 95 °C and midstep temperature of 101 °C is clearly seen in our results. In this work, we will take the onset temperature as the T_g though, in thermal analysis, it is customary to take the midpoint of the step transition as the T_g. We prefer to use the onset because it is established much more unambiguously, as shown in Figure 2, than the midpoint. Also shown in Figure 2 is a heating

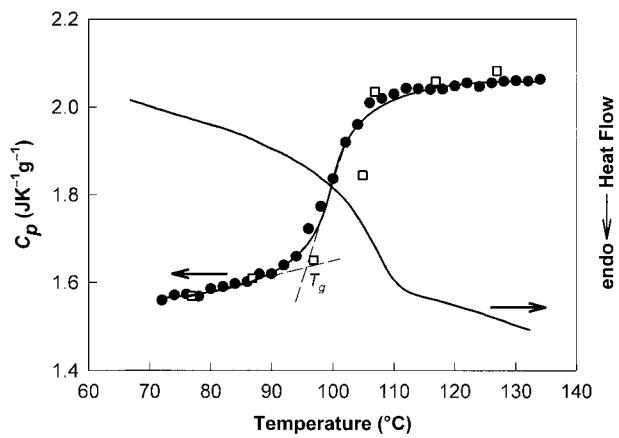

Figure 2. C_p of PMMA as a function of temperature: ●, this work; □, Bu et al.[26] A solid curve is drawn through the data points to elaborate the glass transition. The solid curve pertaining to the heat-flow signal is the DSC scan on PMMA at 5 °C/min. Both C_p measurements and the DSC scan were performed under ambient air pressure.

scan at 5 °C/min on neat PMMA. The T_g, again taken as the onset temperature, obtained from the scan is about 6 °C higher than that obtained from the C_p measurements. This is reasonable because the stepwise heating allows the polymer segments much longer time to relax than the scanning method. A slightly higher T_g is also seen in the literature C_p values shown in Figure 2 as these were also obtained by scanning the sample.

The heat capacity of PMMA-CO_2 under a constant pressure of 34 atm is shown in Figure 3 as a function of temperature. It increases rapidly at temperatures above 50 °C, and goes through a step change similar to that shown in Figure 2. However, this time, the step occurs at a somewhat reduced temperature due to plasticization of PMMA by CO_2, and we identify the transition temperature as $T_{g,h}$. It should be noted that, for the stepwise heating, the holding time at each step (15 min) is comparable with the diffusive time scale of CO_2 in 300-μm thick PMMA and the step-to-step temperature jumps are quite small (1–4 °C). Therefore, the polymer–gas system can be considered to maintain equilibrium during the measurements with the dissolved gas content of the polymer decreasing slightly with each temperature jump. The T_g obtained by the stepwise method thus corresponds to the true gas solubility at the transition temperature. On the other hand, in a scanning run, the temperature changes much faster than the gas diffusive time scale, and the

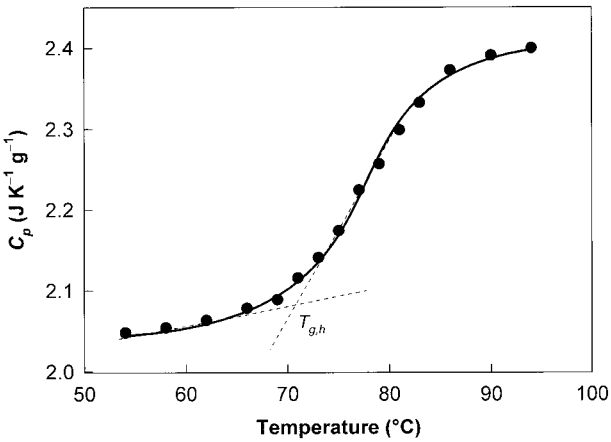

Figure 3. C_p of PMMA-CO_2 solution as a function of temperature under a CO_2 pressure of 34 atm. A solid curve is drawn through the C_p results to elaborate the glass transition.

polymer–gas system is not really in equilibrium. As a result, the plasticized T_g measured by the scanning technique refers to a solubility at a somewhat lower temperature than the glass-transition temperature.

Surprisingly, at low temperatures, the heat capacity of the PMMA-CO_2 system at 34 atm was found to decrease sharply with increasing temperature. The results are shown in Figure 4. This phenomenon was not observed in other polymer–gas systems, such as PS-CO_2 and PS-ethylene, PVC-CO_2, and PETG-CO_2, in which the retrograde vitrification phenomenon has either not been reported or established firmly. Measurements at lower temperatures proved to be quite difficult due to proximity to the condensation conditions of CO_2. The results shown in Figure 4 are for the conditions under which no condensed phase of CO_2 was present in the system. As seen in Figure 4, the heat capacity of the system is unusually high, attaining a value of over 4.5 J K^{-1} g^{-1} at 1.3 °C. The results were quite reproducible, thereby, ruling out the presence of any condensed phase of CO_2. Although the sorption of a small molecules results in an increase in polymer's heat capacity as reported in the literature[27] and as is evident from Figures 2 and 3, the C_p increase in PMMA-CO_2 solution at low temperatures is far beyond the anticipated effect. In view of the retrograde vitrification phenomenon reported in the literature,[18] we assign the observed C_p behavior to the rubber-to-glass transition and identify the $T_{g,l}$ as shown in Figure 4. Such a low-temperature transition, though easily measured by the stepwise method, cannot be detected by the conventional scanning method. This is because, for a given pressure, the difference between the $T_{g,l}$ and the CO_2 condensation temperature is too small to establish a stable baseline in a conventional DSC scan. It should be noted that the C_p change associated with the rubber-to-glass transition shown in Figure 4 is much larger than the corresponding change for the glass-to-rubber transition shown in Figure 3. At low temperatures, the system is very close to the saturation vapor pressure curve of CO_2, and the dissolved CO_2 is in a more liquidlike state.[28] Consequently, it makes a much larger contribution to the C_p of the system than it would under conditions corresponding to the supercritical state of CO_2, which is the case for the results shown in Figure 3.

Thus, by establishing the glass-to-rubber transition temperatures as illustrated in Figure 3 and the rubber-to-glass transition temperatures as illustrated in Figure 4, a complete T_g-p profile for PMMA-CO_2 was generated, and is shown in Figure 5. The $T_{g,l}$ and $T_{g,h}$ curves meet at 43 °C and 58 atm. Also shown in Figure 5 is the saturation vapor pressure curve of CO_2, which runs very close to the $T_{g,l}$ curve. As mentioned above, DSC measurements were also made in the stepwise pressure-scanning mode. A set of typical results is shown in Figure 6 where the heat capacities of the PMMA-CO_2 solution at 26 °C are plotted against the gas pressure. The onset of the transition gives a plasticization pressure p_g of 47 atm. This is in good agreement with a T_g of 26 °C at 49 atm

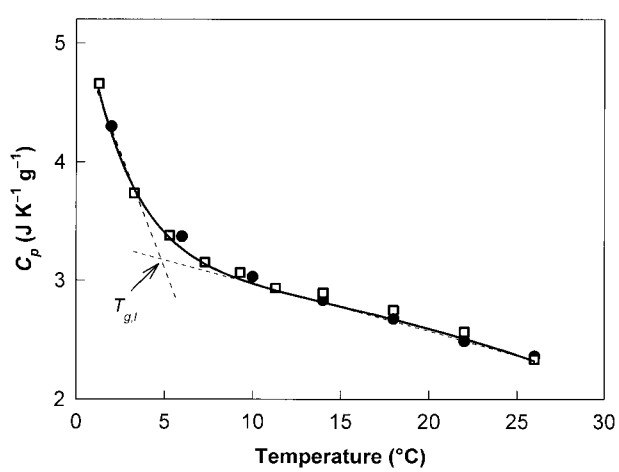

Figure 4. C_p of PMMA-CO_2 solution at low temperatures and a CO_2 pressure of 34 atm. A solid curve is drawn through the C_p results to elaborate the glass transition. ●, first run; □, second run.

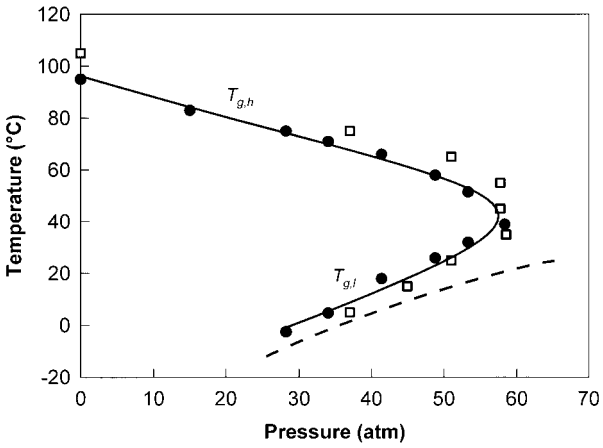

Figure 5. T_g of PMMA-CO_2 plotted against the gas pressure: ●, this work; □, Condo and Johnston.[21] A solid curve is drawn through the data points to show the trend. The vapor–liquid equilibrium boundary for CO_2 is shown by the dashed curve; CO_2 exists as a compressed vapor above this curve and as a compressed liquid below it.

estimated from the results shown in Figure 5. Thus, even though the two techniques give similar results, the stepwise temperature scanning method is the preferred technique as it is about 30 times faster than the stepwise pressure-scanning method.

The result in Figure 5 shows the so-called retrograde vitrification behavior previously reported for this system.[18–21] For example, consider the PMMA-CO_2 system at 40 atm and 2 °C. Then, according to Figure 5, these T, p conditions define a state in-between the CO_2 saturation vapor pressure curve and the $T_{g,l}$ curve. The system under these conditions is in the rubbery state. On heating at 40 atm, the system enters the phase envelope where it exists as a glass. Thus, a rubber transforms to glass on heating or, if the isobaric process is reversed, the glass transforms to rubber on cooling, and this is termed the retrograde vitrification.[18] Another feature of note is that over a certain pressure range, there exist two T_g's at a given pressure. Accordingly, on heating at 40 atm, the system will first undergo a rubber-to-glass transition at about 14.4 °C and then a glass-to-rubber transition at about 67.8 °C.

The retrograde vitrification profile measured here is similar to that reported in the literature based on creep compliance measurements.[21] The literature results are shown in Figure 5. The agreement between the two sets of results is quite good considering the difference in the measurement techniques and in the assignment of the transition temperature. As seen in Figure 5, the window between the glass-transition line, $T_{g,l}$, and the CO_2 condensation line is quite small. This excludes the application of conventional scanning methods in measuring T_g in such polymer–gas systems. Accordingly, the isobaric stepwise temperature scanning technique, the pseudoisothermal stepwise pressure-scanning technique, and the isothermal pressure-scanning technique (creep compliance) are deemed useful for characterizing the retrograde behavior. It is easier to automate the programmed temperature ramping than pressure ramping, and the small thermal mass associated with the DSC vessels allows temperature equilibrium to be established rapidly. In this context, the isobaric stepwise heating method developed here is more efficient and easier to use than the other techniques. It should, however, be noted that the measurements terminate at the point where the $T_{g,l}$ curve intersects the CO_2 condensation curve. Both methods, stepwise thermal analysis and pressure-scanning creep compliance measurements, share this limitation.

Retrograde vitrification is conjectured to occur because of the rather high gas solubility of CO_2 at low temperatures, especially at temperatures below the critical temperature of CO_2.[18] In order to confirm this, the solubility S of CO_2 in PMMA was measured under a constant pressure of 34 atm and at various temperatures. Figure 7 shows the van't Hoff plot of the solubility in the temperature range −0.2–110 °C. A rapid increase in solubility is seen at temperatures below about 9.5 °C. This exceptionally high solubility under conditions

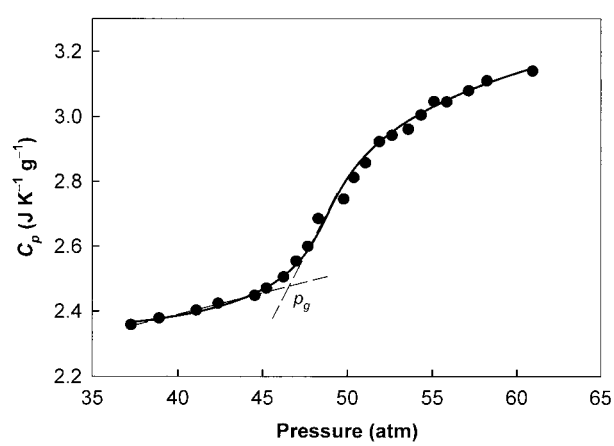

Figure 6. C_p of PMMA-CO_2 solution at 26 °C under various CO_2 pressures. A solid curve is drawn through the C_p results to elaborate the glass transition.

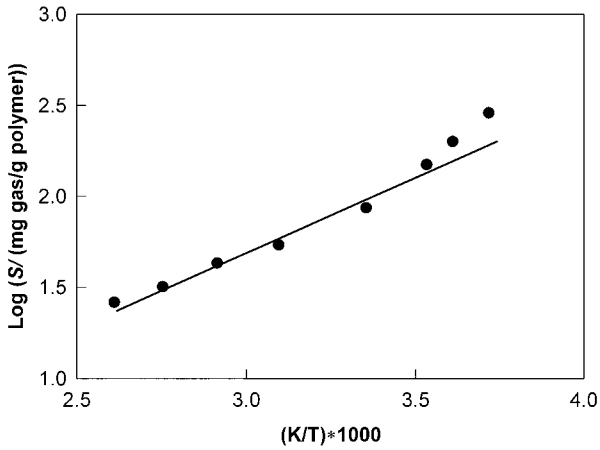

Figure 7. Solubility of CO_2 at 34 atm in PMMA plotted against reciprocal temperature. The solid line represents the van't Hoff fit to the data in the temperature range of about 10 to 110 °C.

where the system approaches the saturation vapor pressure curve of CO_2 was also predicted theoretically.[18,19] This enhanced solubility is, in fact, responsible for the existence of the rubbery state at low temperatures as shown in Figure 5, or conversely, the rapid decrease in solubility on heating the low temperature phase is responsible for the rubber-to-glass transition identified as $T_{g,l}$ in Figure 4. The existence of the rubbery state at low temperatures is further supported by the sorption kinetics results shown in Figure 8; gas sorption occurs more rapidly at −0.2 °C than at 24 °C because of the much faster diffusion of CO_2 at the lower temperature. A detailed investigation on the solubility and diffusivity of CO_2 in PMMA over extended ranges of temperature and pressure is now in progress in our laboratory.

The Effect of Retrograde Vitrification on Foaming

A polymer containing dissolved gas can be foamed by rapidly releasing the gas pressure (called pressure quench method) or by rapidly heating the polymer–gas solution (called the temperature soak method). In either method, the polymer–gas system should be above its plasticized T_g for the foaming to occur. Thus, the T_g-p profile identifies the necessary conditions for foaming. For systems exhibiting retrograde behavior, such as that shown in Figure 5, the pressure quench method will apply when the polymer is saturated with the gas outside the retrograde envelope—the rubbery region—whereas the temperature soak method will apply when the polymer is saturated with the gas or liquid within the retrograde envelope—the glassy region. This has been proven by our experiments under various conditions. In our work, no foams were obtained when the polymer was saturated within the glassy region and then subjected either to pressure quench or heated to within 5 °C of the phase boundary after the pressure was released, whereas a variety of foams could easily be produced from the rubbery phases that exist above $T_{g,h}$ or below $T_{g,l}$.

Other factors, such as the activity of CO_2 and the polymer viscosity, also determine whether cell nucleation and growth will occur or not. For example, at −0.2 °C and 34 atm, although PMMA is in the rubbery state and the gas solubility is quite high, no foaming was observed on pressure quench. This is attributed to the rather poor performance of CO_2 as a blowing agent under conditions close to its saturation vapor pressure curve. However, at slightly elevated temperatures and pressures, 24 °C and 53 atm, PMMA could be easily foamed by simply releasing the gas pressure, and foaming by the pressure quench method occurred most efficiently at pressures above the maximum retrograde pressure $p_{g,\max}$ of 58 atm, or at temperatures above $T_{g,h}$. These observations suggest that high viscosity of the macromolecules and the reduced activity of CO_2 at low temperatures prevent foaming by the pressure quench method. They also suggest that slight heating of the samples saturated under conditions corresponding to the lower end of the $T_{g,l}$ curve should favor foaming. This indeed was found to be the

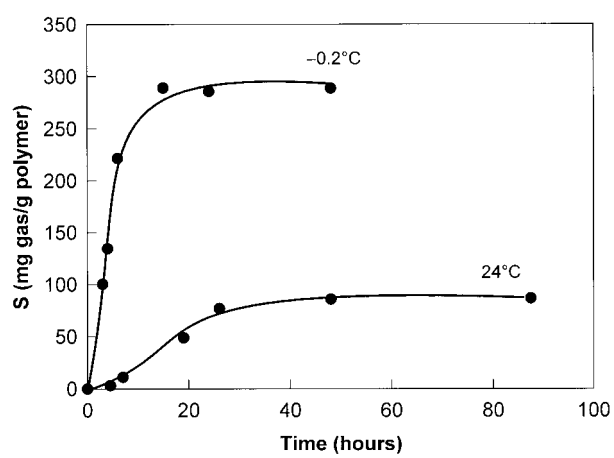

Figure 8. A comparison of the sorption kinetics of 34 atm CO_2 in PMMA at −0.2 °C and 24 °C. Solid curves are drawn through the data points to elaborate the markedly different sorption rates.

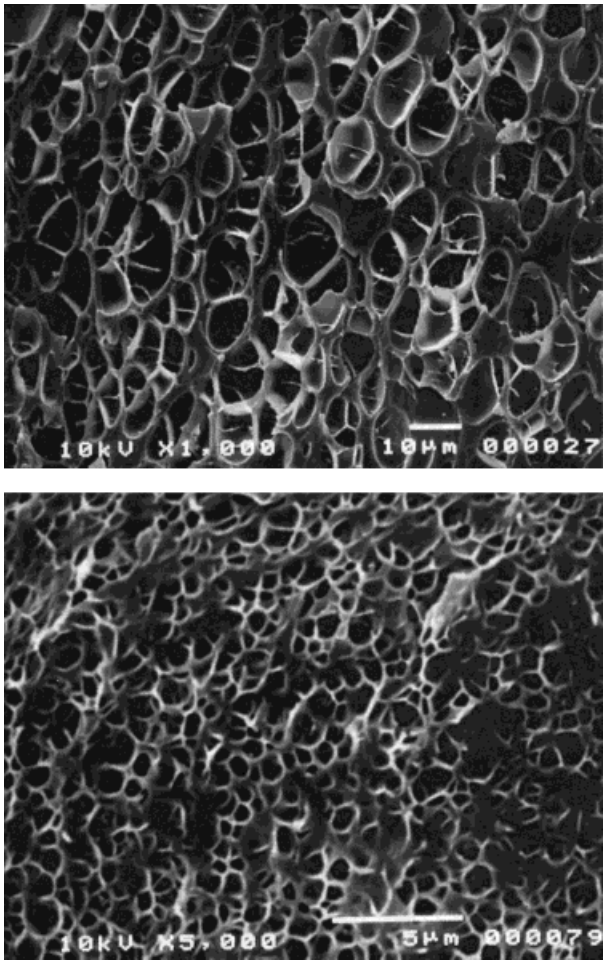

Figure 9. Microphotographs of PMMA foams obtained by saturating the polymer with 34 atm CO_2 at −0.2 °C. Top photograph: foaming temperature 24 °C, average cell size 4.8 μm; bottom photograph: foaming temperature 80 °C, average cell size 0.35 μm.

case. For example, the PMMA sample saturated at −0.2 °C and 34 atm easily foamed when heated to a temperature above 10 °C. As shown in Figure 9, foams with fine closed-cell structure were obtained when such a sample was quickly heated to a temperature in the range 24 to 80 °C.

The retrograde behavior also affects the morphology of the foamed polymer. Foams with cell size less than 5 μm, such as those shown in Figure 9, were obtained only if the polymer was saturated at conditions below the $T_{g,l}$ curve or at temperatures below $T_{g,l}$ and at pressures beyond $p_{g,\max}$. On the other hand, if the polymer was saturated with CO_2 at 24 °C and 34 atm, that is, inside the retrograde envelope, and then heated to 80 °C—a temperature just above the $T_{g,h}$ at 34 atm—closed-cell foams with much larger cells

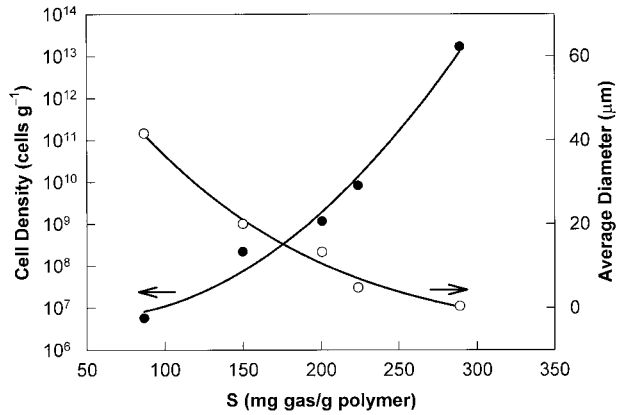

Figure 10. Cell density and average cell size of PMMA foams as a function of CO_2 solubility in the polymer. All samples were foamed at 80 °C. A solid curve is drawn through the data points to show the trend.

(about 40 μm) were obtained, the cell size being about 100 times that shown in Figure 9. It should be noted that PMMA foams with cellular characteristics comparable to those shown in Figure 9 have previously[9,24] been produced at temperatures in the range 30 to 60 °C and at pressures over 130 atm. The latter pressure is much higher (values of 30–50 atm) than the pressures required for producing foams from the retrograde phase.

The effect of saturation conditions on foam morphology can be attributed to the variation of CO_2 solubility with temperature. Figure 10

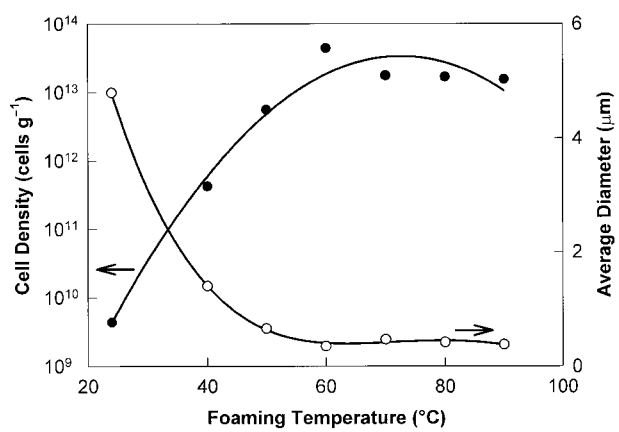

Figure 11. Cell density and average cell size of PMMA foams as a function of foaming temperature. Foam samples were obtained from PMMA saturated with 34 atm CO_2 at −0.2 °C. A solid curve is drawn through the data points to show the trend.

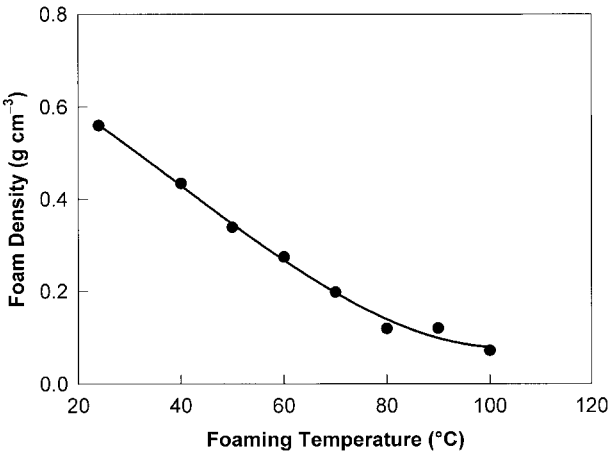

Figure 12. Density of PMMA foams as a function of foaming temperature. Foam samples were obtained from PMMA saturated with 34 atm CO_2 at −0.2 °C. A solid curve is drawn through the data points to show the trend.

shows the dependence of cell density and cell size on CO_2 solubility for the PMMA samples foamed at 80 °C. It is clear that solubility plays a vital role in controlling cell density and cell size. The equilibrium solubility of CO_2 in PMMA is 22.5 wt % at −0.2 °C and 34 atm and decreases rapidly to 7.9 wt % at 24 °C and 34 atm. This gives rise to quite different foam morphologies as reported above. Since exceptionally high gas solubilities can be achieved at conditions below the $T_{g,l}$ curve, micro- and ultramicrocellular foams with unique morphologies can be generated. Figures 11 and 12 show, respectively, the cell density, cell size, and foam density of microcellular PMMA as a function of foaming temperature after the polymer was saturated with CO_2 at −0.2 °C and 34 atm. With increasing temperature, cell nucleation rate increases, resulting in an increase in cell density and reduction in cell size and foam density. The nucleation effect, however, levels off at high temperatures because of cell coalescence. Thus, by optimizing the foaming temperature, PMMA foam with an average cell size of 0.35 μm, cell density of 4.4×10^{13} cells/g, and foam density of 0.116 g/cm^3 can be made after saturating the polymer with CO_2 at −0.2 °C and 34 atm. The production of such an ultramicrocellular structure at low pressures has not been reported in the literature. For example, a minimum cell size of 0.5 μm and a maximum cell density of 10^{12} cells/cm^3 has been reported when PMMA was saturated with CO_2 at 40 °C and 272 atm.[9,29]

The authors thank Mr. Gerry Pleizier and Dr. Jacques Roovers for assistance with the SEM and GPC work, respectively. This study was issued as NRCC No. 42004.

REFERENCES AND NOTES

1. Koros, W. J.; Hellums, M. W. Fluid Phase Equilib 1989, 53, 339.
2. Sasaki, M.; Takishima, S.; Masuoka, H. Proc. International Symposium on Supercritical Fluids, Nice, France, 1988, pp 711–718.
3. O'Neill, M.; Kruus, P.; Pritchard, K.; Handa, Y. P. Proc. 3rd International Symposium on Supercritical Fluids, Strasbourg, France, 1994, pp 345–351.
4. Berens, A. R.; Huvard, G. S.; Korsmeyer, R. W.; Kunig. F. W. J Appl Polym Sci 1992, 46, 231.
5. Kazarian, S. G. Appl Spectrosc Rev 1997, 32, 301.
6. Nealey, P. F.; Cohen, R. E.; Argon, A. S. Macromolecules 1994, 27, 4193.
7. Watkins, J. J.; McCarthy, T. J. Macromolecules 1995, 28, 4067.
8. Handa, Y. P.; Zhang, Z.; Wong, B. Macromolecules 1997, 30, 8499.
9. Goel, S. K.; Beckman, E. J. Polym Eng Sci 1994, 34, 1137.
10. Handa, Y. P.; Wong, B.; Zhang, Z.; Kumar, V.; Eddy, S.; Khemani, K. Polym Eng Sci 1999, 39, 55.
11. Wang, W.-C. V.; Kramer, E. J.; Sachse, W. H. J Polym Sci Polym Phys 1982, 20, 1371.
12. O'Neill, M. L.; Handa, Y. P. Assignment of the Glass Transition. ASTM STP 1249; Seyler, R. J., Ed.; American Society for Testing and Materials: Philadelphia, 1994.
13. Zhang, Z.; Handa Y. P. J Polym Sci Part B: Polym Phys 1998, 36, 977.
14. Banerjee, T.; Lipscomb, G. G. J Appl Polym Sci 1998, 68, 1441.
15. Zhang, Z.; Handa, Y. P. Macromolecules 1997, 30, 8505.
16. Handa, Y. P.; Kruus, P.; O'Neill, M. J Polym Sci Part B: Polym Phys 1996, 34, 2635.
17. Wissinger, R. G.; Paulaitis, M. E. J Polym Sci Part B: Polym Phys 1991, 29, 631.
18. Condo, P. D.; Sanchez, I. C.; Panayiotou, C. G.; Johnston, K. P. Macromolecules 1992, 25, 6119.
19. Kalospiros, N.; Paulaitis, M. E. Chem Eng Sci 1994, 49, 659.
20. Condo, P. D.; Johnston, K. P. Macromolecules 1992, 25, 6720.
21. Condo, P. D.; Johnston, K. P. J Polym Sci Part B: Polym Phys 1994, 32, 523.

22. Mraw, S. C.; Naas, D. F. J Chem Thermodyn 1979, 11, 567.
23. Martini-Vvedensky, J. E.; Suh, N. P.; Waldman, F. U.S. Patent 4,473,665, September 25, 1984.
24. Baldwin, D. F.; Suh, N. P.; Park, C. B.; Cha, S. W. U.S. Patent 5,334,356, August 2, 1994.
25. Fleming, G. K.; Koros, W. J. Macromolecules 1990, 23, 1353.
26. Bu, H. S.; Aycock, W.; Wunderlich, B. Polymer 1987, 28, 1165.
27. Bershtein, V. A.; Egorov, V. M. Differential Scanning Calorimetry of Polymers; Ellis Howood: London, 1994.
28. Koros, W. J.; Paul, D. R. J Polym Sci Polym Phys Ed 1978, 16, 1947.
29. Goel, S. K.; Beckman, E. J. Polym Eng Sci 1994, 34, 1148.